We are IntechOpen, the world's leading publisher of Open Access books Built by scientists, for scientists

6,900
Open access books available

185,000
International authors and editors

200M
Downloads

Our authors are among the

154
Countries delivered to

TOP 1%
most cited scientists

12.2%
Contributors from top 500 universities



WEB OF SCIENCE™

Selection of our books indexed in the Book Citation Index in Web of Science™ Core Collection (BKCI)

Interested in publishing with us?
Contact book.department@intechopen.com

Numbers displayed above are based on latest data collected.
For more information visit www.intechopen.com



16

Projecting Changes in Extreme Precipitation in the Midwestern United States Using North American Regional Climate Change Assessment Program (NARCCAP) Regional Climate Models

Shuang-Ye Wu
University of Dayton, USA

1. Introduction

Based on the physics of global circulation, many expect an enhanced greenhouse effect to lead to a more active hydrological cycle with more precipitation on average (Hennessy et al. 1997). This expected increase has been found in observations (Zhang et al. 2007) and has also been suggested by climate models, although these models are not consistent with respect to the spatial and temporal variability about this change. An increase in mean precipitation depth, assuming no change in the shape of the frequency distribution, would imply an increased frequency of heavy-precipitation events. However, some studies (Hennessy et al. 1997, Allen and Soden, 2008) also suggest the increase in these extreme events could be disproportionate to the change in the mean, with a greater fraction of the total precipitation being delivered by such heavy precipitation events. Such a shift towards heavy events is a common conclusion of climate models (Cubasch et al. 2001, Meehl et al. 2007) as well as analyses of observed rainfall data at the continental scale (Easterling 2000, Kunkel 2003, Groisman 2005, Min et al. 2011). However, there is great spatial variation of this average pattern. This study aims to establish likely future projections for how extreme precipitation frequency and magnitude could change in the Midwestern region of the United States, and investigate the spatial variation of such changes within the area.

Present global climate models (GCMs) typically produce results at the spatial resolution of 150-300 km. This level of spatial resolution of GCMs is insufficient for establishing localized future climate projections and examining their spatial variations at the scale of a state. For increased spatial resolution, we used a set of Regional Climate Models (RCMs) run by National Center for Atmospheric Research (NCAR) under the North American Regional Climate Change Assessment Program (NARCCAP). RCMs involve nesting a higher resolution climate models within a coarser resolution GCM. The GCM output is used to define boundary conditions around a limited domain, within which RCM further models the physical dynamics of the climate system. These RCMs are designed to produce high resolution climate change simulations in order to investigate uncertainties in regional scale

projections of future climate and generate climate change scenarios for use in regional and local impacts research (Mearns et al, 2009).

This study aims to achieve two main objectives. First, we evaluate the performance of NARCCAP models in terms of whether they capture the frequency distribution of daily precipitation data. This evaluation is based on a comparison of retrospective model runs with observed station-based daily precipitation data. Second, based on the evaluation, we correct the bias in mean precipitation and frequency distribution of precipitation output from RCMs. After the model biases have been corrected, we then project future changes of mean and extreme precipitation patterns in the Midwest Region.

2. The Midwestern Region

The definition of the Midwestern region of the USA differs in literature. The Midwestern U.S. defined for the National Climate Change Assessment program (Easterling and Karl, 2000) includes the upper eight states south of the Great Lakes (Figure 1). We expanded the region to include Kentucky because of its similarities in both physical and socio-economic characters to the rest of the region. Based on 2010 census, the nine states contain about 21% of the nation's population. Their cumulative gross state product is approximately 20% of national gross domestic product of 2010. Therefore it is an area of great economic importance. Situated at the heart of the Corn Belt, the region's economy is dominated by farming, with 89% of the land area being used for agricultural purposes. As a result, climate variability and extreme weather play a key role in the economic productivity of the region. In recent decades, the Midwest region has observed a noticeable increase in average temperatures despite the strong year-to-year variations (Union of Concerned Scientists, 2009). The largest increase has occurred in winter. Both summer and winter precipitation has been above average for the last three decades, making it the wettest period in a century. Heavy rainfall events are also significantly more frequent than a century ago. The Midwest has experienced two record-breaking floods in the past 15 years (Union of Concerned Scientists, 2009). It can be seen from these already observed changes that climate change will have a profound impact on the region. As a result it is very important to investigate how precipitation pattern will change for the region in the near future.

The Midwestern region has a typical continental climate, although the Great Lakes have a great influence on nearby areas for both temperature and precipitation. The total annual precipitation of the region averages at 950 mm (1895-2005). In fall and winter, the precipitation is largely produced by mid-latitude wave cyclones. In spring and summer, it is dominated by varying amount of convective thunderstorm rainfall. In most part of the region, precipitation is highly seasonal, with most of the rainfall concentrated in spring and summer. However in the Ohio River Valley in the southeastern part of the region, the amount of precipitation is fairly constant throughout the year. Spatially, annual precipitation ranges from 600 mm in northwest to 1200 mm in southeast, because of the increasing proximity to the Gulf of Mexico source of moisture (Figure 1). The slight deviation to this precipitation gradient is leeway shores of the Great Lakes, where lake effect precipitation, particularly from August to December, generates relatively wet conditions that lead to an annual precipitation depth around 900 - 1000 mm (Huff and Angel, 1992). Most of extreme precipitation events occur in spring and summer. Heavy precipitation in spring, when evaporation is relatively low due to lower temperature, can lead to severe flooding.

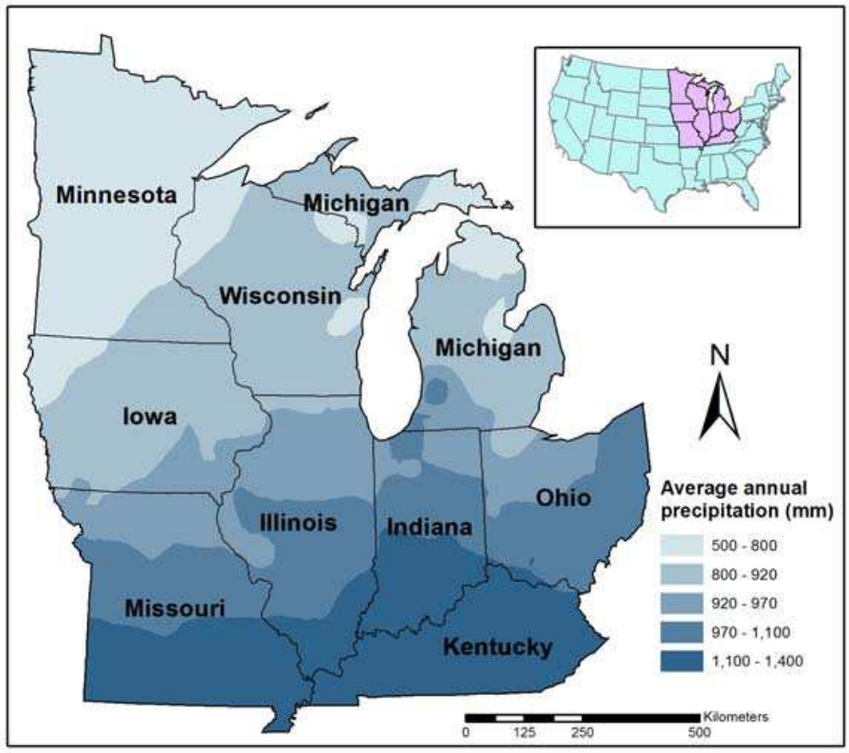


Fig. 1. Study area: annual mean precipitation in the Midwest United States

3. Data and methodology

3.1 Data

For model evaluation, observed daily precipitation data 1971-2000 were obtained from US Historical Climatology Network (USHCN) for climate stations in the Midwest Region. The time period was selected because it was the temporal domain of retrospective runs carried out by NARCCAP RCMs. We excluded years with less than 350 days of records to preserve frequency distribution of the data series, and any station with less than 25 complete years of records. We finally had 204 stations, with an average of 28.5 complete years of record per station.

NARCCAP includes 6 RCMs driven by 4 GCMs over the domain of North America, and they typically have the spatial resolution of 50 km. Not all simulations are completed. At the time of this study, 6 of the 24 RCM-GCM combinations are finished and data distributed. Table 1 shows the RCM-GCM combinations used in this study. For model evaluation, we used RCM retrospective runs (1971-2000), which produce 3-hourly precipitation data series. This data was summarized into daily precipitation data series 1971-2000. For projecting future precipitation patterns, we summarized RCM output for 2040-2070 into future daily precipitation data series. All model runs are driven with A2 emission scenario defined by the Intergovernmental Panel on Climate Change (IPCC) Special Report on Emission Scenarios (SRES) (IPCC, 2000). A2 assumes a medium high level of CO_2 emission based on a development pattern close to business-as-usual.

RCMs	GCMs			
	CCSM	CGCM3	GFDL	HADCM3
CRCM		X	X	
MM5I	X			
HRM3				X
RCM3		X		
WRFG	X			

Table 1. GCM-RCM combinations used in this study

3.2 Model evaluation methodology

In order to examine the frequency and magnitude of extreme events, it is important for a model to capture an accurate distribution of the data series. We first computed and compared the statistics that describe the shape of distribution for observed and modeled daily precipitation data. We chose to use L-moments to characterize the frequency distributions based on methods developed in Hosking (1990). L-moments are similar to conventional moments in that they are calculated to summarize the shape of a probability distribution. L-mean is identical to the conventional mean, whereas L-scale, L-skewness and L-kurtosis are analogous to conventional standard deviation, skewness and kurtosis. L-moments however are often considered superior to conventional moments in characterizing distribution shapes, because they are less sensitive to outliers (Ulrych et. al, 2000, Elamir et.al, 2003, and Hosking 2006).

We then attempted to quantify the deviation of the distributions of daily data output from 6 NARCCAP RCMs from observed daily precipitation distribution based on the following steps:

- Establish the empirical cumulative distribution function (F_{obs}) for observed precipitation series for each station: x_i , $i=1,2\ldots n$

$$F_{obs}(t) = \frac{1}{n}\sum_{i=1}^{n} 1\{x_i \le t\} \tag{1}$$

  Where 1{A} is the indicator function of event A.
- Based on F_{obs}, calculate the probability (p) for each observed precipitation value P_j

$$p(P_j) = F_{obs}(P_j) = \frac{1}{n}\sum_{i=1}^{n} 1\{x_i \le P_j\} \tag{2}$$

- Find the corresponding value in the modeled daily precipitation data for the grid point closest to that station (P_j^m) that has the same probability. That is, calculate the quantile (Q^m)value at p in the modeled precipitation data series

$$P_j^m = Q^m(p(P_j)) = x^m_{\lceil n_m p(P_j)\rceil} \tag{3}$$

  Where n_m is the number of data points in the modeled precipitation data series; x^m is the sorted modeled precipitation data series where $x_1^m \le x_2^m \ldots \le x_n^m$; $\lceil\rceil$ is the ceiling function.

- Calculate the model error (E) for each station as the root mean squared difference between P_j and P_j^m

$$E = \sqrt{\frac{\sum_{j=1}^{n}(P_j - P_j^m)^2}{n}} \tag{4}$$

Based this method, we evaluated E for complete precipitation data series, as well as the error for observed dry days (E_d) and wet days (E_w) separately at each climate station. We then calculated the mean error for all stations in the state for each model.

3.3 Method for projecting future mean and extreme precipitation

A Common approach to studying extreme events is to establish their probability distributions, upon which the magnitude and return intervals (frequency) of extreme events can be established. This can be achieved either by fitting a theoretical distribution functions, or based on the empirical distribution of the data. The advantage of using theoretical distributions is that they can smooth out outliers, particularly when data is only available for short time frame, and they can project beyond the time period when data is available.

Before we can apply this approach, however, we need to correct biases of RCMs in the frequency distribution of their output daily precipitation data series (as evaluated based on the methods outlined in 3.2). It is important to correct the entire distribution, not just mean values. We propose a quantile mapping method to achieve this correction.

3.3.1 Bias correction through quantile mapping

This involves the following steps:

- Establish an empirical cumulative distribution function (F_{mf})for modeled future daily precipitation data series x_i^{mf}

$$F_{mf}(t) = \frac{1}{n}\sum_{i=1}^{n} 1\{x_i^{mf} \le t\} \tag{5}$$

- For each modeled future precipitation value P_j^{mf}, find the corresponding quantile values of same probability in the observed and modeled current daily precipitation data series: P_j^{obs} and P_j^{mc}

$$P_j^{obs} = Q^{obs}(F_{mf}(P_j^{mf})) = x^{obs}_{\lceil n_{obs}F_{mf}(P_j^{mf})\rceil} \tag{6}$$

Where n_{obs} is the number of data points in the observed precipitation data series; x^{obs} is the sorted observed precipitation data series where $x_1^{obs} \le x_2^{obs} \ldots \le x_i^{obs}$.

$$P_j^{mc} = Q^{mc}(F_{mf}(P_j^{mf})) = x^{mc}_{\lceil n_{mc}F_{mf}(P_j^{mf})\rceil} \tag{7}$$

Where n_{mc} is the size of the modeled current precipitation data series; x^{mc} is the sorted modeled current precipitation data series where $x_1^{mc} \le x_2^{mc} \ldots \le x_i^{mc}$.

- We then use the ratio of P_j^{obs} and P_j^{mc} to correct the bias in future precipitation data series.

$$\hat{P}_j^{mf} = P_j^{mf} \frac{P_j^{obs}}{P_j^{mc}} = P_j^{mf} \frac{x^{obs}_{\lceil n_{obs} F_{mf}(P_j^{mf}) \rceil}}{x^{mc}_{\lceil n_{mc} F_{mf}(P_j^{mf}) \rceil}} \tag{8}$$

Based on this bias-correction, we derived a future daily precipitation data series from RCMs for each of the climate station.

3.3.2 Frequency analysis

After the bias in the distribution is corrected, we then fit a theoretical distribution function to both the observed and future modeled data, based on which the magnitude of precipitation events of certain return intervals can be established for comparison. A variety of distribution functions have been used to study extreme precipitation events, such as generalized extreme value (GEV), Weibull and Pearson III distributions for annual maxima data, generalized Pareto (GP) distribution for excesses over a high threshold, and generalized Logistic (GL), lognormal (LN) and Gamma distributions for full precipitation records. We used the L-moment ratio (L-skewness vs. L-kurtosis) diagram (Rao and Hamed, 1999) to help select the best distribution for our data. Figure 2 plot the L-skewness and L-kurtosis ratios for both observed and modeled data for all stations. Results show that Gamma distribution best approximate the distribution of daily precipitation totals. This selection is also supported by many previous studies (Crutcher et al. 1977, Buishand 1978, Guttman et al. 1993, Groisman et al. 1999). Gamma distribution has the following density function:

$$f(x) = \frac{1}{\alpha^{\beta}\Gamma(\beta)} x^{\beta-1} e^{-(\frac{x}{a})} \tag{9}$$

The variable x has lower bound of zero, $0 < x < \infty$. For this family of distributions, the α-parameter defines the shape of the distribution, while β-parameter characterizes the scale. Since it does not rain every day, a mixed distribution model is sometimes considered for daily precipitation totals (Groisman et al, 1999). Under this model, it is assumed that the occurrence of daily precipitation events has a binary distribution with the probability of a single event p_{pr}, and the precipitation amount during this event is considered to have a gamma-distribution. The cumulative distribution function of precipitation totals $F(x)$ is expressed as:

$$F(x) = P(X \le x) = (1 - p_{pr}) + p_{pr} \int_0^x f(\alpha, \beta, t) dt \tag{10}$$

with $f(\alpha,\beta,t)dt$ being the probability density function of gamma-distribution. p_{pr} can be estimated as the percentage of wet days in the data series. The maximum likelihood method is used to estimate the parameters α and β for each of the observed and future modeled

daily precipitation data series. After the cumulative probably density function $F(x)$ is established we can derive the magnitude of precipitation events of various return intervals as:

$$P_y = F^{-1}(1 - \frac{1}{365y}) \tag{11}$$

Where P_y is the precipitation value with the return interval of y years, $F^{-1}(x)$ is the inverse function of the cumulative probability function $F(x)$.

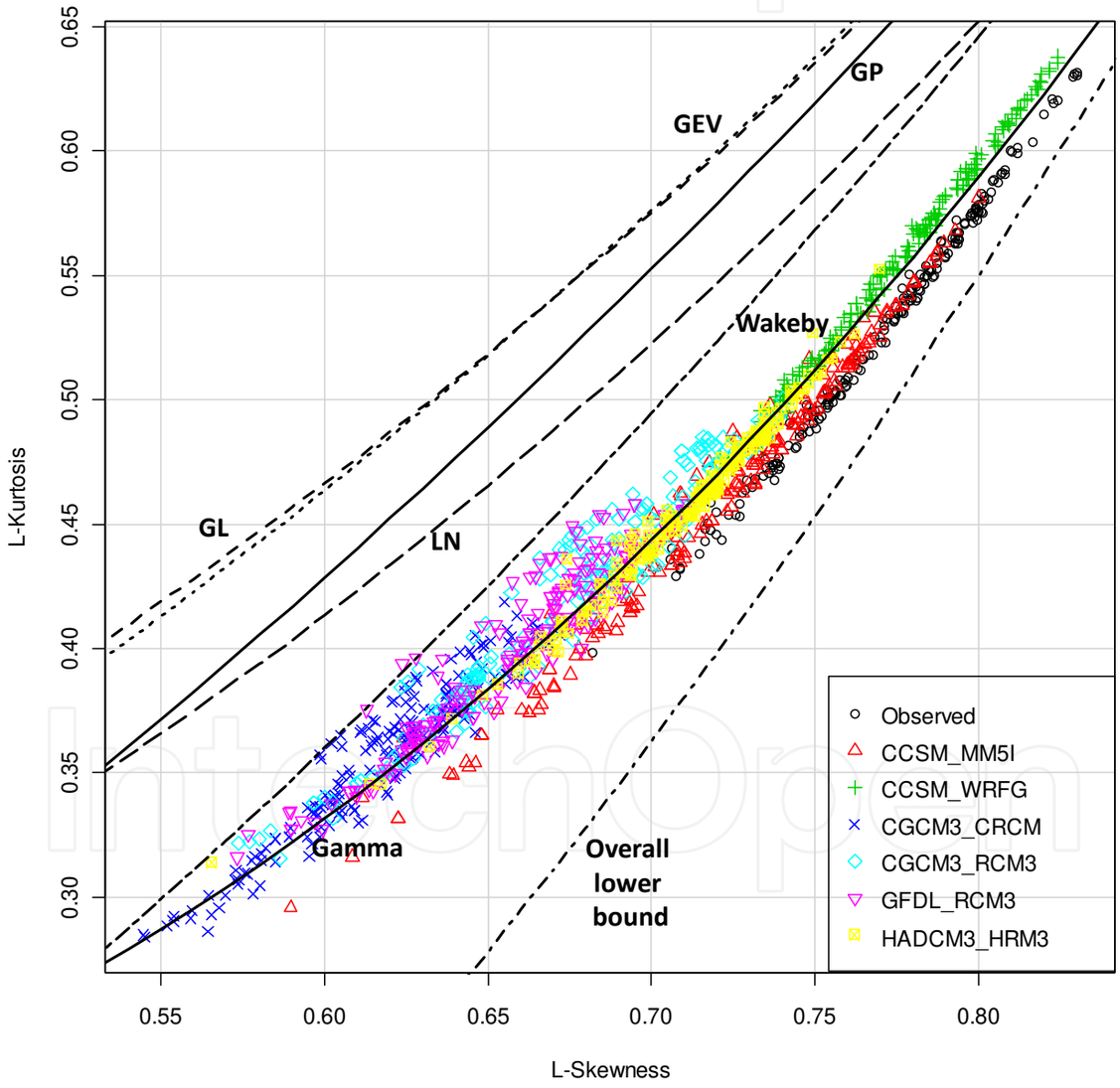


Fig. 2. L-moment ratio diagram for observed and modeled daily precipitation data in comparison to the L-moment ratio curves of theoretical distributions

4. Results and discussions

4.1 Model evaluation: Frequency distributions of observed and modeled daily precipitation data

Summary L-moment statistics for frequency distributions of observed and modeled daily precipitation data series are presented in Table 2. It can be seen that CCSM_WRFG daily precipitation series deviate most from the observed distribution of daily precipitation. The remaining models have comparable biases. They all have greater mean (except for CCSM_MM5I), less variance, skewness and kurtosis. This seems to indicate that the modeled data is less spread out, have higher values in small precipitation events and lower values in large events (hence less skewed than observed).

Figure 3 illustrates the correlation between observed and modeled mean daily precipitation at all stations. The correlation coefficient (Pearson's r) values are also presented in the figure. It should be noted that to evaluate a model's performance at estimating mean precipitation, we should not only look at the correlation coefficient, but also how closely the points follow the x=y line. It can be seen that CCSM_WRFG model consistently under-estimate the mean daily precipitation. Most models slightly over estimate the mean daily precipitation (such as CGCM_RCM3, GFDL_RCM3 and HADCM3_HRM3). The model that performs best in terms of mean precipitation is CGCM3_CRCM, which has the highest correlation coefficient (0.81), and follows x=y line most closely. However, close estimate in mean precipitation does not mean the model also simulates well the whole distribution of daily precipitation data series. Figure 4 presents the quantile-quantile (Q-Q) plots between observed and modeled data for all stations for each of the 6 RCMs in order to show the deviation from observed distribution as well as the spread of different models. It can be seen from figure 4 that despite its close estimate of mean precipitation, CGCM3_CRCM performs the worst in estimating the complete distribution. It consistently underestimates most of the wet day quantile values. The close estimate of the mean is a result of over-estimation of small precipitation events offsetting this underestimation of larger quantile values. Figure 4 shows that majority of models underestimate large quantile values. All models overestimate days with no or small amount of precipitation. This can also be illustrated by the dry day quintile errors (E_d) presented in table 3. To some extent, this could be attributable to the fact that RCMs output average precipitation of a whole grid, which covers an area of 50 by 50 km, whereas station data are point-based.

Table 3 summarizes root mean squared error of modeled quantile values for all data (E), dry days (E_d) and wet days (E_w) respectively. Based on RMSE, it seems that HADCM3_HRM3 performs best in estimating the observed frequency distribution of daily precipitation data, as it has lowest E and E_w, and fairly low E_d. The calculated model errors again confirm that CCSM_WRFG and CGCM3_CRCM have the poorest performance in simulating the frequency distribution, and its model errors are above the other models. The rest of the models have comparable performance. The average RMSE for full record quantiles for all models is about 1 mm, or about 40% of mean precipitation amount. This ranges from 0.78 to 1.65 mm, or 30 to 63% of mean daily precipitation. The average RMSE for wet day quantile values for all models is 3.04 mm, or 35% of the mean wet day precipitation. It ranges between 25-54% of mean wet day precipitation among different models.

Model	Mean (mm/day)		L-scale		L-skewness		L-kurtosis	
	Value	% diff.	Value	% diff.	Value	% diff.	Value	% diff.
Observed	2.62		0.88		0.77		0.53	
CCSM_MM5I	2.40	-8.38	0.84	-3.58	0.72	-6.18	0.46	-12.05
CCSM_WRFG	1.96	-25.39	0.87	-0.73	0.77	0.14	0.55	4.17
CGCM3_CRCM	2.65	0.92	0.76	-13.28	0.62	-19.55	0.36	-32.03
CGCM3_RCM3	3.09	18.01	0.80	-8.28	0.67	-12.36	0.42	-19.97
GFDL_RCM3	2.90	10.52	0.79	-9.56	0.66	-14.52	0.40	-24.14
HADCM3_HRM3	2.95	12.49	0.83	-4.94	0.71	-7.71	0.46	-13.37
Model mean	2.66	1.36	0.82	-6.73	0.69	-10.03	0.44	-16.23

Table 2. Summary statistics for frequency distributions of observed and modeled daily precipitation data series

Model	E	E as % of mean daily precipitation	E_d	E_w	E_w as % of mean wet day precipitation
CCSM_MM5I	0.93	36	0.07	2.95	34
CCSM_WRFG	1.11	42	0.05	3.63	42
CGCM3_CRCM	1.65	63	0.36	4.65	54
CGCM3_RCM3	0.85	32	0.27	2.16	25
GFDL_RCM3	1.02	39	0.29	2.69	31
HADCM3_HRM3	0.78	30	0.15	2.18	25
Model mean	1.06	40	0.20	3.04	35

Table 3. Root mean squared error of modeled quantile values for all data (E), dry days (E_d) and wet days (E_w)

4.2 Projecting future precipitation patterns in the Midwest Region

4.2.1 Mean daily precipitation

After applying bias correction based on quantile mapping method, we calculated future mean daily precipitation for the Midwest region for the time period 2040-2070. Table 4 summarizes how daily mean precipitation might change for the study area based on climate models. With the exception of CCSM_WRFG (which projects very slight decrease), all other models project increase in mean precipitation in the region. The average change for all models is 7.7%, ranging from 0-12%. Figure 5 shows the spatial pattern of precipitation change based on mean projection of all models. It seems that mean precipitation is likely to increase more in north and less in the south. This is likely due to increased evaporation from the Great Lakes under a warmer temperature. Spatial pattern of mean precipitation change varies among different models (Figure 6), but most models project increase in the northern part of the region. CCSM_WRFG is the only model that project decrease of precipitation in the south at the similar magnitude as the increase in the north. All other models project increase in all Midwest region.

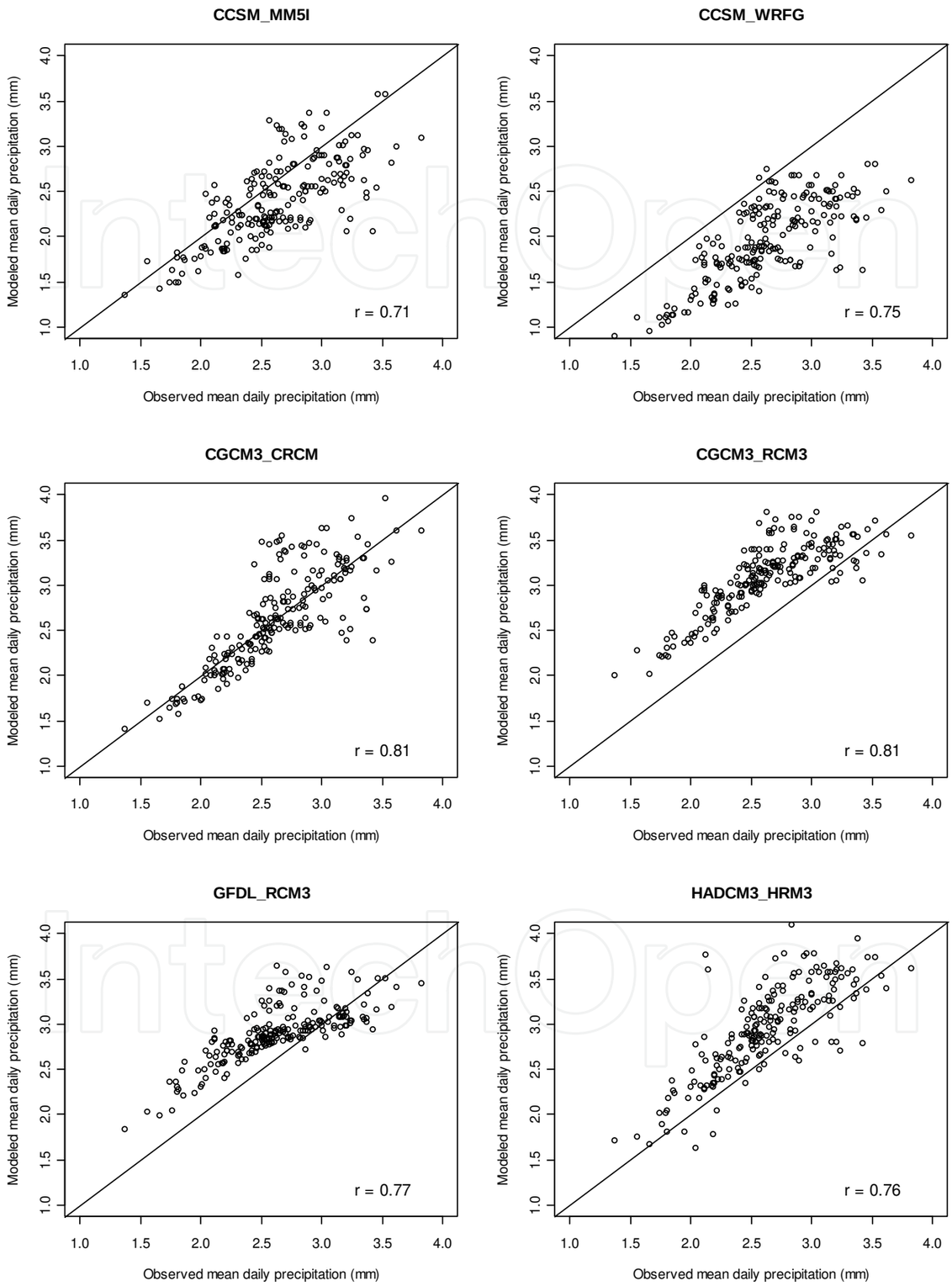


Fig. 3. Correlation between observed and modeled mean daily precipitation at all stations.

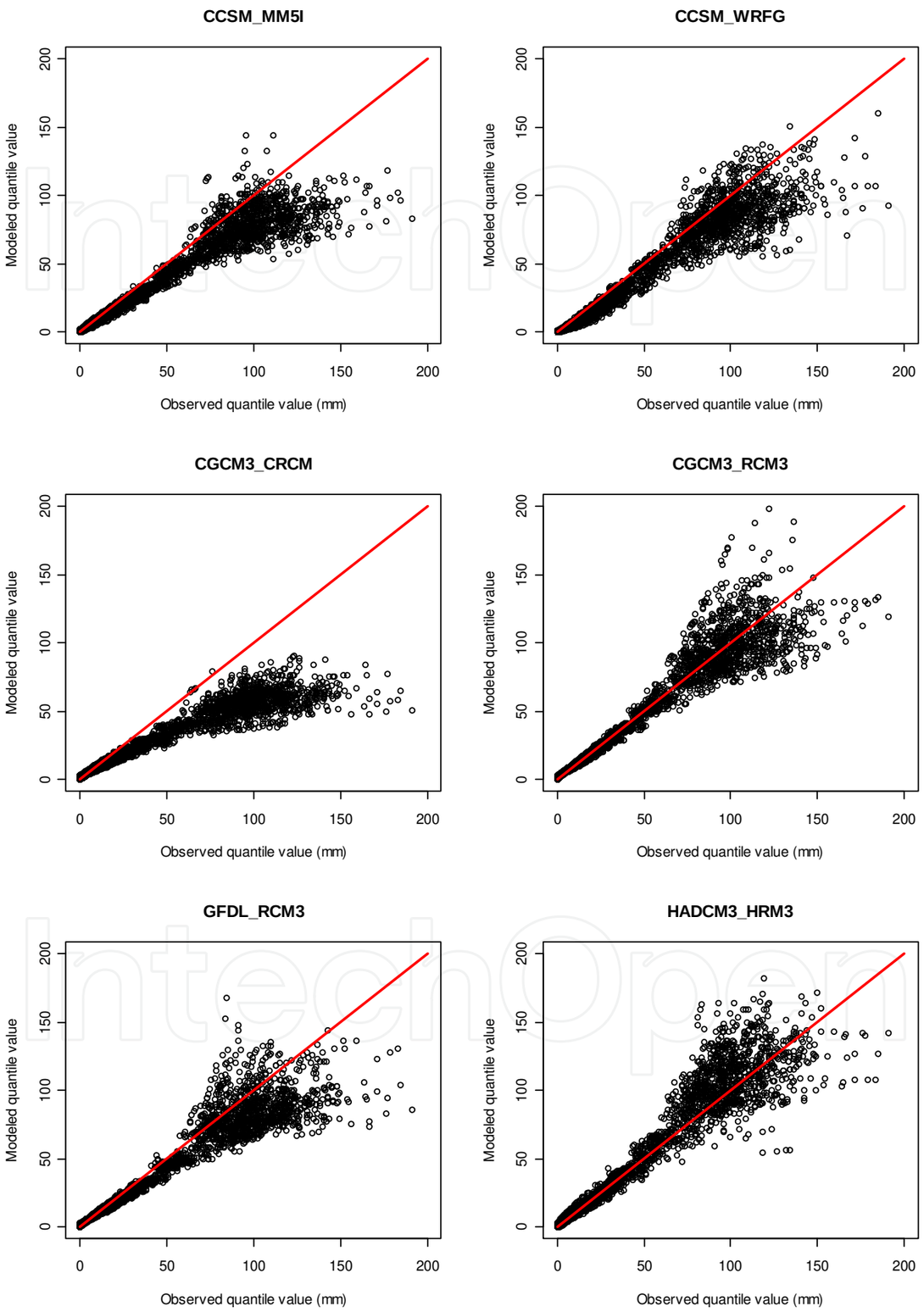


Fig. 4. Q-Q plots for all stations for each of the RCMs

Models	Mean daily precipitation (mm/d)	% change
Observed (1971-2000)	2.62	
Future (2040-2070)		
CCSM_MM5I	2.87	9.51
CCSM_WRFG	2.61	-0.44
CGCM3_CRCM	2.79	6.59
CGCM3_RCM3	2.89	10.11
GFDL_RCM3	2.86	8.95
HADCM3_HRM3	2.93	11.67
Model mean	2.82	7.73

Table 4. Changes in the Midwest mean daily precipitation in 2040-2070

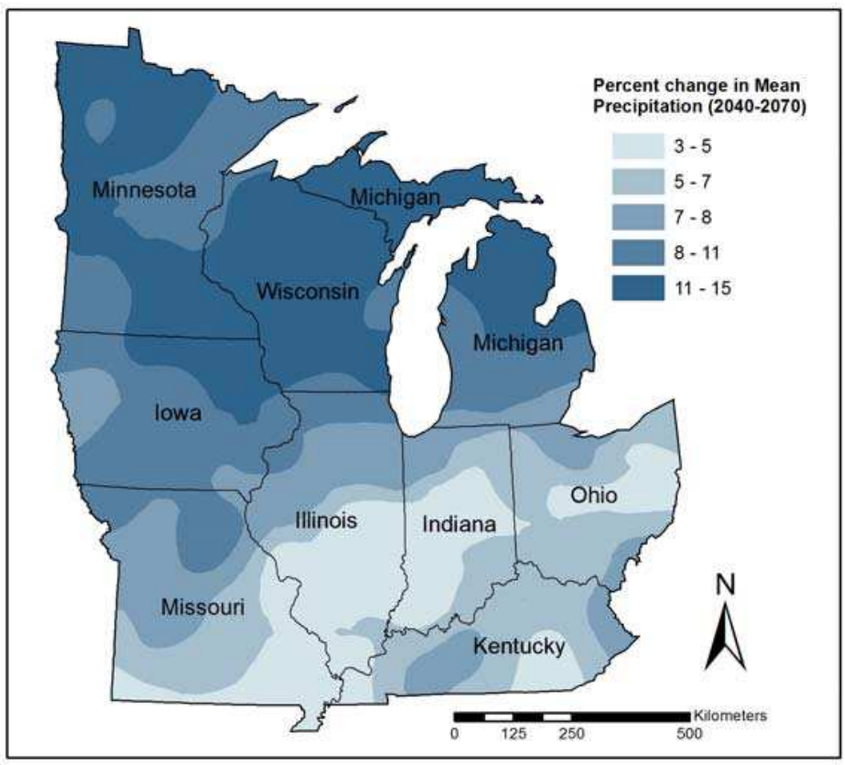


Fig. 5. Changes in mean daily precipitation in 2040-2070 (model mean).

4.2.2 Extreme precipitation events

We used the mixed probability model (eq. 10) to project extreme precipitation events. We used the wet day frequency as an estimate for precipitation probability (p_{pr}), and fit a Gamma distribution to the wet day precipitation data using maximum likelihood method. Applying the same methodology on the observed and bias-corrected future daily precipitation data, we derived the magnitudes of extreme events of return interval of 1, 5, 10, 15, 20 and 25 years for both present (1970-2000) and future (2040-2070). Table 5 summarized the results. All models show increase in precipitation depths of extreme events. In general, extreme precipitation events increase at greater magnitudes than mean precipitation. The increase is greater for more extreme events. For average results of all models, compared with 8% increase in mean precipitation, precipitation event of 1 year return interval is likely to increase by 13%, and that of 25 year could increase by 19%. There are variations among models in how they project spatial distribution of such changes. Our model evaluation suggests that mean of all models seems to capture the spatial variation of precipitation best. Based on this observation, we used mean values of all models to interpolate the spatial distribution of how extreme precipitation could change in the Midwest (Figure 7). It can be seen that in general the intensity for extreme precipitation increase disproportionately

Return interval		**1 year**	**5 year**	**10 year**	**15 year**	**20 year**	**25 year**
Observed (1970-2000)	mm/day	55	82	96	103	108	112
Future (2040-2070)							
CCSM_MM5I	mm/day	62	93	108	117	124	128
	% change	12.59	13.26	13.19	13.72	14.51	14.70
CCSM_WRFG	mm/day	62	93	108	116	124	129
	% change	11.80	12.70	12.90	12.87	14.31	14.86
CGCM3_CRCM	mm/day	61	91	106	114	121	125
	% change	9.90	10.96	10.94	10.86	11.82	12.11
CGCM3_RCM3	mm/day	64	100	117	127	135	141
	% change	16.11	20.86	22.45	23.21	24.98	25.69
GFDL_RCM3	mm/day	61	94	111	122	132	137
	% change	9.72	13.61	16.01	18.56	21.43	22.76
HADCM3_HRM3	mm/day	64	98	114	126	134	139
	% change	15.94	19.44	19.48	22.15	23.75	24.37
Model mean	mm/day	62	95	111	120	128	133
	% change	12.68	15.14	15.83	16.90	18.47	19.08

Table 5. Present and future magnitudes of extreme precipitation events.

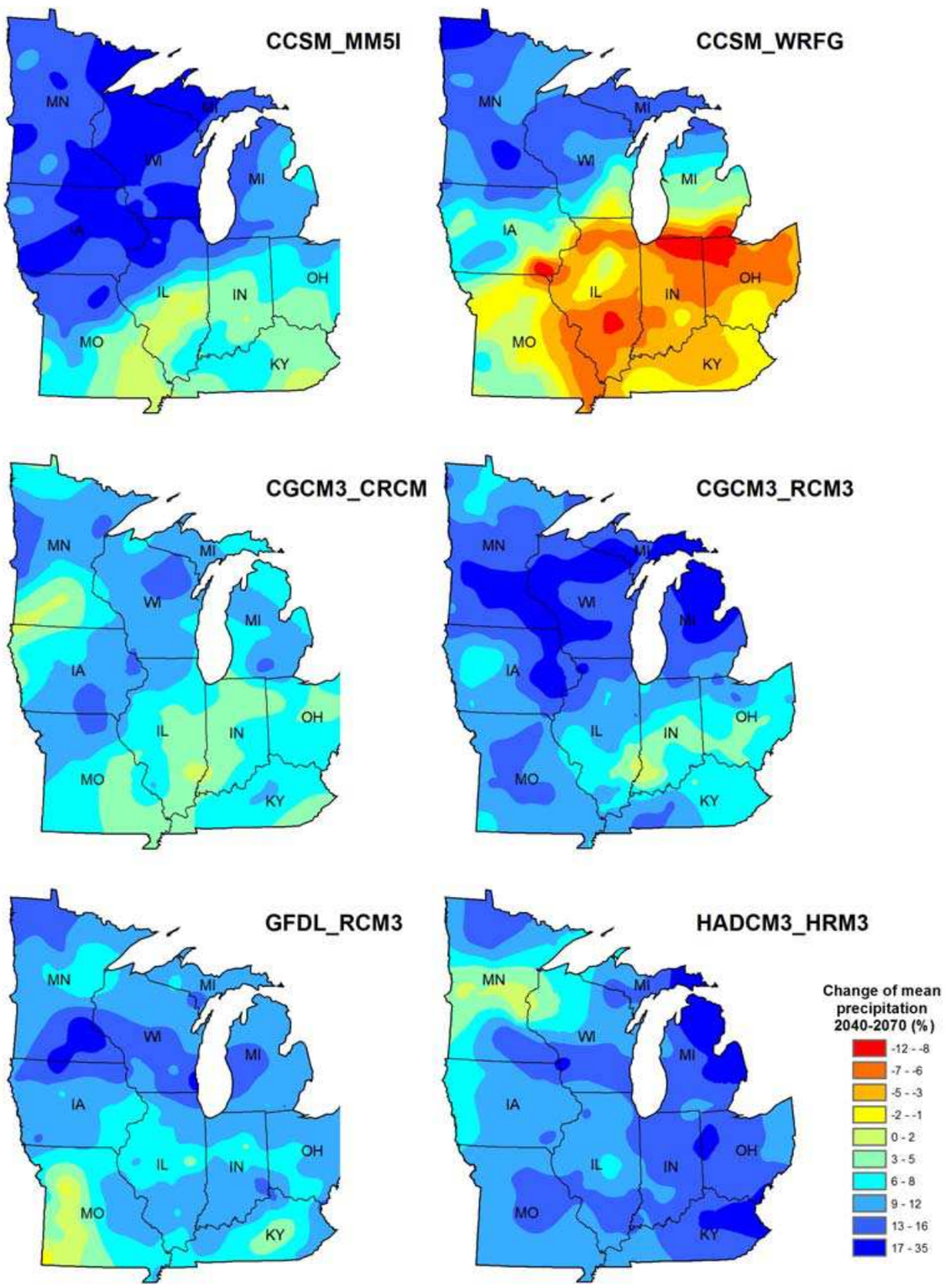


Fig. 6. Changes in mean daily precipitation in 2040-2070 from 6 RCMs

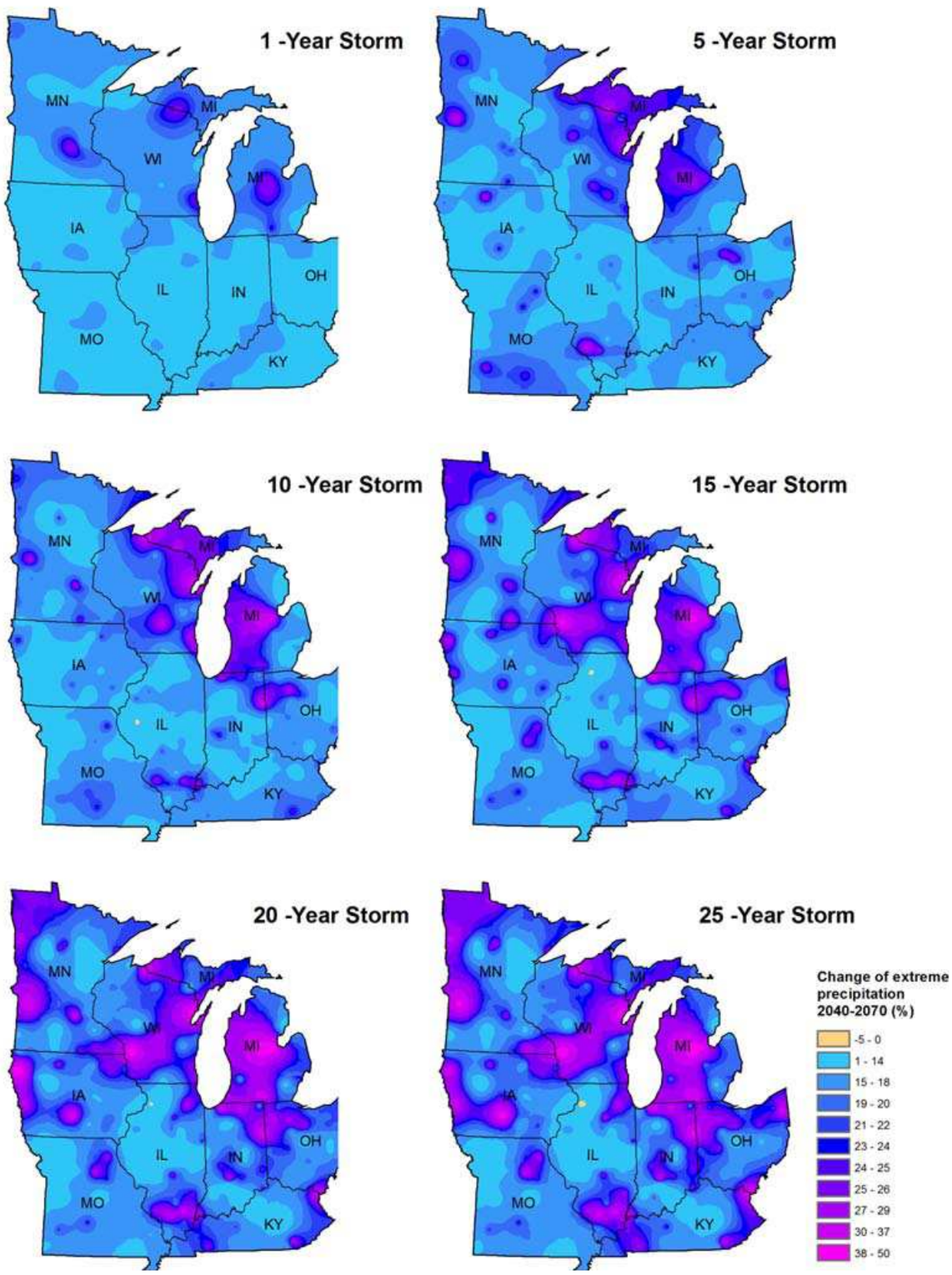


Fig. 7. Changes in extreme precipitation (2040-2070).

more for more extreme events. Similar to the pattern of mean precipitation change, there seems to be more increase in extreme events in the northern part of the region. Since a lot of extreme precipitation events occur in spring, this increase could be attributed to decreased ice cover during the winter, early melt of lake ice, and consequent increased evaporation of the great lakes under a warmer climate.

5. Conclusion

In this study, we first evaluated the performance of NARCCAP regional climate models in terms of its ability to capture the frequency distribution of daily precipitation data in the Midwest region of the United States. We found all models have biases. In general, they tend to overestimate small events, and underestimate large events. Based on such evaluation, we corrected model biases based on quantile-mapping method. We then used the bias-corrected future daily precipitation output from NARCCAP RCMs to project future changes in precipitation using a mixed probability model based on Gamma distribution. Based on the models, on average, the mean precipitation could increase by 7.7% by 2040-2070 for the Midwestern Region. Magnitudes of extreme precipitation are likely to increase more than average. The increase could be disproportionately larger for more extreme precipitation events. Spatially, northern part of the study area could see more increase in both mean and extreme precipitation, likely due to increased evaporation of the Great Lakes from a combination of higher temperature and less ice cover both spatially and temporally under a warmer climate.

6. References

Allan RP, Soden B J. 2008. Atmospheric warming and the amplification of precipitation extremes. *Science* 321:1481–1484.

Buishand, TA. 1978. Some remarks on the use of daily rainfall models. *Journal of Hydrology*, 36:295-308.

Crutcher, HL, McKay, GF, Fullbright, DC. 1977. A note on a gamma distribution computer program and computer produced graphs. NOAA Technical Report EDS24, Environmental Data Service, NOAA, Department of Commerce, Washington DC.

Cubasch U, Boer GJ, Stouffer RJ, Dix M, Noda A, Senior CA, Raper S, Yap KS. 2001. Projections of future climate change, in *Climate Change 2001: The Scientific Basis. Contribution of Working Group I to the Third Assessment Report of the Intergovernmental Panel on Climate Change.* Edited by J.T. Houghton et al., pp. 525-582. Cambridge University Press, New York.

Easterlin DR and Karl TR. 2000 Potential consequences of climate variability and change for the Midwestern United States. In *Climate Change Impacts on the U.S.: The Potential Consequences of Climate Variability and Change*, ed. National Climate Assessment Team, p 167-188.

Easterling DR, Evans JL, Ya P, Groisman PY, Karl TR, Kunkel KE, Ambenje P. 2000. Observed variability and trends in extreme climate events: a brief review. *Bulletin of the American Meteorological Society* 81(3): 417-425.

Elamir, EAH, Seheult, AH. 2003. "Trimmed L-moments". *Computational Statistics & Data Analysis* 43 (3): 299–314. doi:10.1016/S0167-9473(02)00250-5.

Groisman PY, Karl TR, Easterling DR, Knight RW, Jamason, PF, Hennessy, KJ, Suppiah, R. Page, CM, Wibig, J, Fortuniak, K, Razuvaev VN, Douglas A. Forland, E, Zhai PM. 1999. Changes in the probability of heavy precipitation: Important indicators of climate change. *Climatic Change* 42:243-283.

Groisman PY, Knight RW, Easterling DR, Karl TR, Hegerl GC, Razuvaev VN. 2005. Trends in intense precipitation in the climate record. *Journal of Climate* 18:1326-1350.

Guttman, NB, Hosking, JRM, Wallis, JR. 1993. Regional precipitation quantile values for the Continental United States computed from L-moments. *Journal of Climate*, 6:2326-2340.

Hennessy KJ, Gregory JM, Mitchel JFB. 1997. et al. 1995. Changes in daily precipitation under enhanced greenhouse conditions. *Climate Dynamics* 13: 667-680.

Hosking JR. 1990. L-moments: analysis and estimation of distributions using linear combinations of order statistics. *Journal of Royal Statistical Society B*, 52: 105-124.

Hosking, JRM. 2006. "On the characterization of distributions by their L-moments". *Journal of Statistical Planning and Inference* 136: 193–198.

Huff, FA, Angel JR. 1992. *Rainfall Frequency Atlas of the Midwest*. Midwestern Climate Center Bulletin 71.

Intergovernmental Panel on Climate Change. 2000. Special Report on Emission Scenarios. UN Environment Program, Nairobi, Kenya.

Kunkel KE. 2003. North American trends in extreme precipitation. *Natural Hazards* 29: 291–305.

Mearns LO, Gutowski WJ, Jones R, Leung L-Y, McGinnis S, Nunes AMB, and Qian, Y. 2009. A regional climate change assessment program for North America. *EOS* 90(36): 311-312.

Meehl GA, Stocker TF, Collins WD, Friedlingstein P, Gaye AT, Gregory JM, Kitoh A. Knutti R, Murphy JM, Noda A, Raper SCB, Waterson IG, Weaver AJ, Zhao Z-C. 2007. Global climate projections. In: *Climate Change 2007: The Physical Science Basis. Contribution of Working Group I to the Fourth Assessment Report of the Intergovernmental Panel on Climate Change.* Edited by S. Solomon et al. pp. 749-845. Cambridge University Press, New York.

Min SK, Zhang X, Zwiers FW, Hegerl GC. 2011 Human contribution to more-intense precipitation. *Nature* 470:378-381. doi:10.1038/nature09763.

Rao, AR, Hamed KH. 2000 *Flood Frequency Analysis.* CRC Press, Boca Raton, Florida.

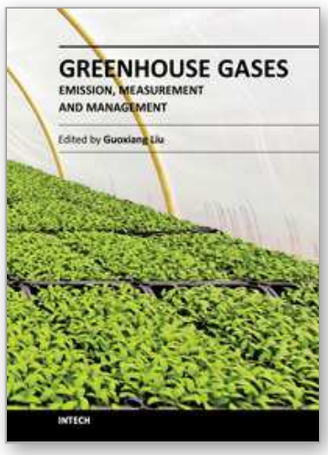
Ulrych, T J, Velis, DR, Woodbury, AD, Sacchi, MD. 2000. "L-moments and C-moments". *Stochastic Environmental Research and Risk Assessment*, 14 (1), 50–68.

Union of Concerned Scientists. 2009. Confronting Climate Change in the U.S. Midwest. http://www.ucsusa.org/global_warming/science_and_impacts/impacts/climate-change-midwest.html. Accessed Nov. 1, 2011.

Zhang X, Zwiers FW, Hegerl BC, Lambert FG, Gillett NP, Solomon S, Stott PA, Nozawa T. 2007. Detection of human influence on twentieth-century precipitation trends. *Nature* 448: 461-465. doi:10.1038/nature06025

IntechOpen

IntechOpen



Greenhouse Gases - Emission, Measurement and Management
Edited by Dr Guoxiang Liu

ISBN 978-953-51-0323-3
Hard cover, 504 pages
Publisher InTech
Published online 14, March, 2012
Published in print edition March, 2012

Understanding greenhouse gas sources, emissions, measurements, and management is essential for capture, utilization, reduction, and storage of greenhouse gas, which plays a crucial role in issues such as global warming and climate change. Taking advantage of the authors' experience in greenhouse gases, this book discusses an overview of recently developed techniques, methods, and strategies: - A comprehensive source investigation of greenhouse gases that are emitted from hydrocarbon reservoirs, vehicle transportation, agricultural landscapes, farms, non-cattle confined buildings, and so on. - Recently developed detection and measurement techniques and methods such as photoacoustic spectroscopy, landfill-based carbon dioxide and methane measurement, and miniaturized mass spectrometer.

How to reference
In order to correctly reference this scholarly work, feel free to copy and paste the following:

Shuang-Ye Wu (2012). Projecting Changes in Extreme Precipitation in the Midwestern United States Using North American Regional Climate Change Assessment Program (NARCCAP) Regional Climate Models, Greenhouse Gases - Emission, Measurement and Management, Dr Guoxiang Liu (Ed.), ISBN: 978-953-51-0323-3, InTech, Available from: http://www.intechopen.com/books/greenhouse-gases-emission-measurement-and-management/future-changes-in-precipitation-pattern-in-the-midwest-region-of-usa

INTECH
open science | open minds

InTech Europe
University Campus STeP Ri
Slavka Krautzeka 83/A
51000 Rijeka, Croatia
Phone: +385 (51) 770 447
Fax: +385 (51) 686 166
www.intechopen.com

InTech China
Unit 405, Office Block, Hotel Equatorial Shanghai
No.65, Yan An Road (West), Shanghai, 200040, China
中国上海市延安西路65号上海国际贵都大饭店办公楼405单元
Phone: +86-21-62489820
Fax: +86-21-62489821

© 2012 The Author(s). Licensee IntechOpen. This is an open access article distributed under the terms of the Creative Commons Attribution 3.0 License, which permits unrestricted use, distribution, and reproduction in any medium, provided the original work is properly cited.

IntechOpen

IntechOpen